J. Min. Metall. Sect. B-Metall. 60 (3) (2024) 317 - 327

Journal of Mining and Metallurgy, Section B: Metallurgy

EFFECT OF ROTATION RATES ON DISSOLUTION BEHAVIOR OF LIME IN $CaO-Fe_tO-SiO_2-MgO$ SYSTEM

C. Jia [a], Q.-Q. Mou [b], Y. Yu [c], R. A. Muvunyi [a], M.-X. Zhang [a], J.-L. Li [a, c, *]

[a] Hubei Provincial Key Laboratory for New Processes of Ironmaking and Steelmaking, Wuhan University of Science and Technology, Wuhan, Hubei, China
[b] CNCEC-EEC Dajiang Environmental Protection Technology Co., LTD., Huangshi, Hubei, China
[c] Key Laboratory for Ferrous Metallurgy and resources utilization of Ministry of Education, Wuhan University of Science and Technology, Wuhan, Hubei, China

(Received 19 July 2024; Accepted 22 October 2024)

Abstract

For the converter steelmaking process, incompletely dissolved lime will exist in steel slag in the form of f-CaO, which reduces the utilization rate of metallurgical slag and causes the waste of resources. It is extremely important to reduce the production of f-CaO in steel slag and promote the rapid and sufficient dissolution of lime. This paper is based on the early and middle stages of the converter slag-forming route based on the CaO component. The dissolution rate of lime in four different slags was measured by rotating rod method. The evolution behavior of the lime-slag interface and the change behavior of the lime dissolution rate were studied by X-ray diffractometer and an electron probe micro-analyzer. The experimental results show that CaO-FeO solid solutions and (Ca, Mg, Fe) olivine are formed when lime reacts with molten slag at 1400°C. When the FeO content decreases, CaO reacts with the calcium-magnesia-silica to form a high melting point and dense $2CaO·SiO_2$ layer. In addition, at different rotation rates, a $3CaO·SiO_2$ phase layer is formed between the CaO-FeO solid solution layer and the C_2S layer. As the rotation rate increases, the dissolution rate of lime also increases and the mass transfer coefficient reaches the maximum at a rotation rate of 180 rpm. The maximum values are $20.54×10^{-6}$ m/s, $7.86×10^{-6}$ m/s, $9.38×10^{-6}$ m/s, $5.53×10^{-6}$ m/s, respectively.

Keywords: *Lime; Reaction interface; $2CaO·SiO_2$; Dissolution rate; Mass transfer*

1. Introduction

Improving the utilization rate of metallurgical slag is an important means to reduce carbon emissions and improve energy utilization rate. Lime is one of the most frequently used and most important slagging raw materials in the process of converter steelmaking. Generally, 10 ~ 15 kg of lime is consumed per ton of steel. In the production process, due to various complex reasons, the lime is not completely dissolved, but remains in the form of f-CaO in the steel slag [1]. The large amount of accumulated steel slag also leads to environmental harm and loss of resources.

The rapid slagging and dissolution of lime has always been a very important part of the converter steelmaking process. In order to reduce the formation of *f*-CaO, it is necessary to improve the dissolution rate and utilization rate of lime. Li Yuanzhou [2] et al. studied the dissolution rate of solid lime in CaO-MgO(=7.4%-8.0%)-Fe_tO-SiO_2 slag system on the premise of controlling the diffusion mechanism during the lime dissolution process. The lime mass transfer coefficient in the slag and the factor equation of CaO mass transfer when t = 1400°C ~ 1600°C and $CaO/SiO_2 \leq 2.0$ were calculated, and the lime dissolution equation for the reference of producers was proposed. Mengxu Zhang [3] et al. studied the dissolution of active lime in $CaO-SiO_2-Fe_tO-MgO$ slag system at different times, and found that when quicklime reacted with slag, CaO-FeO solid solutions, (Ca, Mg, Fe) olivine at 1400°C, and low melting point calcium-magnesium-silicate minerals of MgO were formed. When the FeO content decreased, CaO reacted with the calcium-magnesium-silicate minerals to form a high melting point and dense $2CaO·SiO_2$ layer. Xia Yunjin [4] et al. studied the dissolution behavior of calcium oxide particles in the slag of

Corresponding author: jli@wust.edu.cn

https://doi.org/10.2298/JMMB240719026J

$CaO-FeO-SiO_2-P_2O_5$ system, and found that when the slag contained P_2O_5, the formation of the lime interface was not C_2S but C_2S-C_3P, and the formation of the solid solution layer of C_2S-C_3P also hindered the lime dissolution. Nobuhiro [5] et al. also found that when lime was dissolved in slag, a dense $2CaO{\cdot}SiO_2$ layer would be formed at the reaction interface. The C_2S layer had a great influence on the dissolution of lime, but the density of the C_2S layer had little influence on the dissolution of lime.

It can be seen that the formation of C_2S solid solution layer deteriorates the kinetic conditions of lime dissolution. As a result, the amount of lime that is not completely dissolved in the converter slag increases. This is also an important factor affecting the utilization rate of metallurgical slag. Generally speaking, the dissolution rate of lime is related to its physical structure and the properties of the slag [4, 6-8]. The lime with small particle size and high porosity has a larger specific surface area, which can increase the reaction area with slag and accelerate the dissolution effect. The same effect can be achieved by changing the composition of the slag or changing the fluidity of the slag. In order to further study the dissolution process of lime, in this paper the slag fluidity is changed during the dissolution of lime based on the different components of the slag in the slag forming route based on the CaO component in the early and middle stages of converter smelting. Based on the detailed data of lime dissolution rate and interface reaction, the mechanism of lime dissolution and the reaction interface evolution when lime is dissolved in converter slag is expounded. This provides a theoretical basis for improving the utilization rate of slag in converter slagging.

2. Experiment

In this study, the lime utilized was obtained through the calcination of limestone. The composition of the limestone was determined via XRF (Thermo Scientific, ARL 9900) analysis. The main component of the limestone was $CaCO_3$, the content was 98.55%, and contained a small amount of MgO, SiO_2 and other components. The slag system studied in this experiment was the composition of the $CaO-Fe_tO-SiO_2$-MgO system in the early and middle stages of the slag forming route based on the CaO component in the converter steelmaking. The slag was formulated by using analytical reagents for CaO, SiO_2, and MgO, with Fe_tO being substituted with ferrous oxalate dihydrate ($C_2H_4FeO_6$). The composition of the slag is detailed in Table 1.

The experiment process was divided into four steps, namely the preparation of the lime cylinder, the synthesis of the slag, the dissolution of the lime and the detection of the sample. The specific process was as follows:

Table 1. *Chemical composition ratio of slag (wt.%)*

Slag	CaO	SiO_2	Fe_tO	MgO
A1	17	40	35	8
A2	20	44	28	8
A3	26	38	28	8
A4	37	39	16	8

The first step was the preparation of the lime cylinder. A cutting machine was uesd to cut the block limestone into a cylinder with a height and diameter of 15 mm, washed it and put it into a vacuum drying oven at 200°C. Carbon tube furnace was used as the experimental equipment, and the specific device schematic diagram was shown in Figure 1. The carbon tube furnace was fed with high purity nitrogen (99.999%, 10 L/min) as a protective atmosphere, and the temperature was raised to 1350°C. The limestone cylinder was placed in a molybdenum basket and subjected to calcination in the constant temperature zone of furnace for 10 min, followed by removal for cooling in order to prepare the lime cylinder.

The second step was the preparation of slag. Analytical reagents were weighed and mixed according to the compositions in Table 1 to obtain slag. The slag was put into a corundum crucible for compaction and the corundum crucible was put into the constant temperature zone of the carbon tube furnace. Then, the furnace was heated to 1100°C under a protective atmosphere of high purity nitrogen. After 30 min, the crucible was taken out and cooled to room temperature to obtain the pre-melting slag. At this time, $C_2H_4FeO_6$ in the slag was decomposed into Fe_tO, and H_2O, CO and CO_2 gases were released, which helped to reduce the volume of the slag and eliminate the splashing behavior of the slag in the lime dissolution experiment.

The third experiment was the lime dissolution experiment. 100 g of pre-melting slag was put into a magnesia crucible. The crucible was placed in the constant temperature zone of the carbon tube furnace, and the protective gas and cooling water were opened. Then the furnace was heated to 1400°C for 5 min to ensure that the slag was completely melted. After that, the lime cylinder was put into the slag, and the stirrer was opened, with the stirring rates set to 75 rpm, 110 rpm, 145 rpm and 180 rpm, respectively. After dissolving for 90 s, the remaining lime particles were removed and air cooled to room temperature.

Finally, the lime sample was tested. Crushed the dissolved lime particle sample and use an inlay

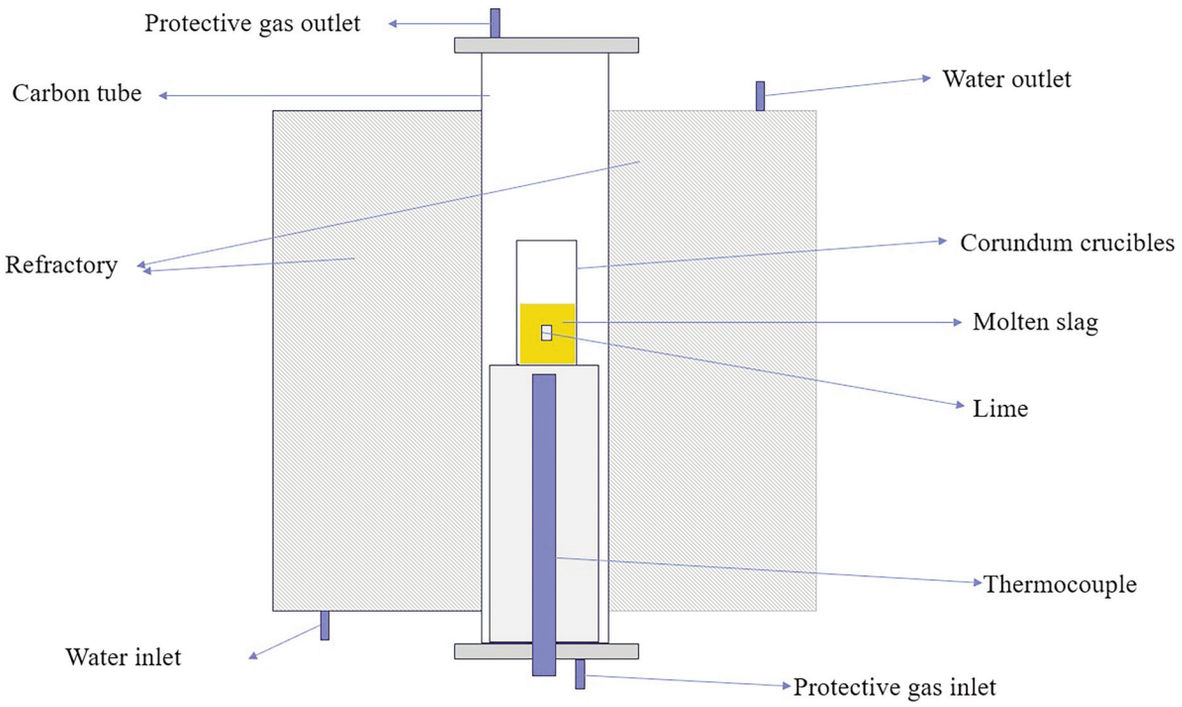

Figure 1. *Schematic diagram of the experiment device*

machine to embed the appropriate lime sample into the metallographic mosaic. Further gold spraying was required on the surface of the embedded sample. Then scanning electron microscopy (SEM) was used to observe the morphology of the reaction interface between the lime and slag. Electron probe micro-analyzer (EPMA 8050G) was used to observe the microscopic morphology of the lime samples, and EDS spectrometer (AZtecLive UltimMax 40) was used to determine the micro-composition, and ImageJ was used to measure the average thickness of each phase layer in the slag.

3. Results

Figure 2 shows the micro-morphology of the lime-slag dynamic reaction interface when lime and slag reacted dynamically at 1400°C for 90 s at different rotation rates. As can be seen from Figure 2, when lime reacted with slag at different rotation rates, a stratification was formed at the reaction interface. The main phase layers were the CaO-FeO solid solution layer, the C_2S layer and the (Ca, Mg, Fe) olivine layer. In addition, new C_3S phase layers were formed between the CaO-FeO solid solution layer and (Ca, Mg, Fe) olivine layer at the lime-slag reaction interface at different rotation rates.

The average thickness of the solid solution layer at the reaction interface changed with the increase of the rotation rate as shown in Figure 3. In slag A1, the thickness of the solid solution layer initially decreased and then increased with the increase of the rotation rate, and when the rotation rate was 180 rpm, there was no solid solution layer, as the high rotation rate strengthens the mass transfer and accelerates the reaction, making it difficult to generate the solid solution layer. In slags A2 and A3, the average thickness of the solid solution layer changed in a similar way, showing a slow decrease at first and then increase. However, in the slag A4, when the rotation rate was 75 rpm and 110 rpm, there was no obvious solid solution layer. When the rotation rate was 145 rpm, the thickness of the solid solution layer was the maximum. According to the morphology of the lime-slag microscopic interface, as shown in Figure 4, when the rotation rate was 75 rpm, the lime did not react with the slag, but presented an overfired state and there was no reaction interface. When the rotation rate was 110 rpm, there were a few solid solution particles at the reaction interface, which proved that the rotation rate accelerated the mass transfer and made the slag react with the lime. In the slag A1 and A2, the thicknesses of solid solutions were the largest when the rotation rate was 75 rpm, and amounted to 16.41 μm and 22.98 μm, respectively. In the slag A3, the thickness of the solid solution generated at 180 rpm was the largest, 18.12 μm. The minimum thicknesses of the solid solutions in slags A2 and A3 were 1.55μm and 13.93 μm respectively when the rotation rate was 145 rpm.

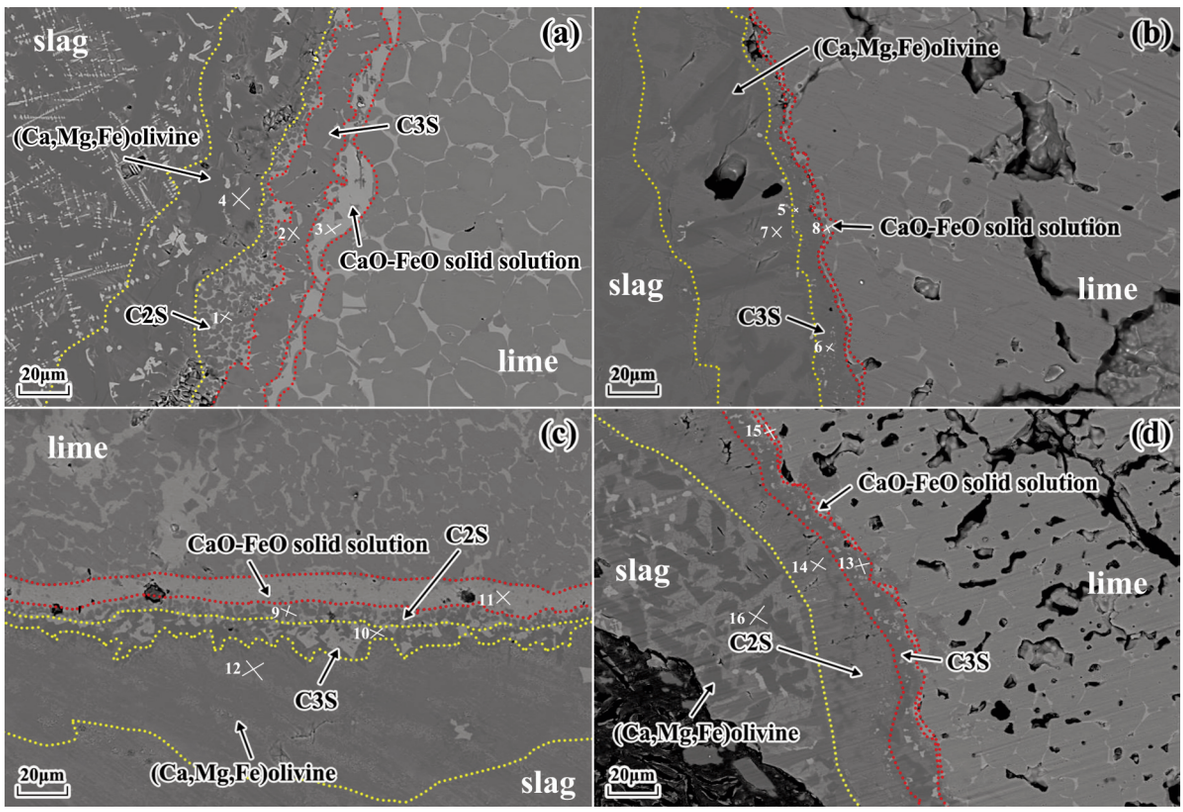

Figure 2. *The microscopic morphology of the reaction interface when the dynamic reaction of lime and slag is 90 s at 1400°C under different rotation rates;*
(a) A1, 110 rpm; (b) A2, 145 rpm; (c) A3, 75 rpm; (d) A4, 180 rpm

Table 2. *EDS point scanning results of reaction interface*

	O	Si	Fe	Ca	Mg
1	50.5	16.3	0.7	31.7	0.8
2	49.7	12.4	1.0	36.1	0.9
3	46.9	0.9	24.6	26.4	1.2
4	49.7	16.8	1.3	24.7	7.6
5	48.3	15.9	4.2	30.6	1.0
6	48.5	12.6	1.1	36.5	1.2
7	47.0	17.8	7.8	17.1	10.3
8	45.3	2.4	23.0	26.2	1.1
9	45.5	17.6	1.4	35.0	0.5
10	49.4	12.3	1.5	35.9	0.8
11	41.6	0.5	28.6	28.2	1.1
12	44.4	19.6	11.2	19.5	5.3
13	48.3	11.5	2.6	32.2	5.4
14	49.8	16.2	0.7	31.8	1.5
15	45.9	2.3	21.7	28.4	1.7
16	45.1	18.8	1.3	17.5	17.3

When lime and slag reacted dynamically at 1400°C at different rotation rates, the average thickness of the (Ca, Mg, Fe) olivine layer generated at the lime-slag reaction interface changed with the increase of the rotation rate, as shown in Figure 5. The (Ca, Mg, Fe) olivine layer was only present in some slags at partial rotation rates. This was due to the improvement of the kinetic conditions and the acceleration of the mass transfer reaction, so that the (Ca, Mg, Fe) olivine layer was reduced. In slag A1, the average thickness of the (Ca, Mg, Fe) olivine layer increased with the increase of rotation rate, and the maximum thickness reached 56.75 μm at a rotation rate of 145 rpm. However, at a rotation rate of 180 rpm, there was no obvious olivine layer in the reaction interface between slag A1 and lime. The slag A1 was the primary slag with good fluidity, and the driving force of CaO was the largest, which was the most suitable for the reaction. Therefore, the (Ca, Mg, Fe) olivine layer and the solid solution layer were not found in the reaction interface at this time. In slag A2, a (Ca, Mg, Fe) olivine layer was found only at a rotation rate of 75 rpm, with an average thickness of 57.32 μm. In slag A3, similar to slag A1, there was no obvious (Ca, Mg, Fe) olivine layer at

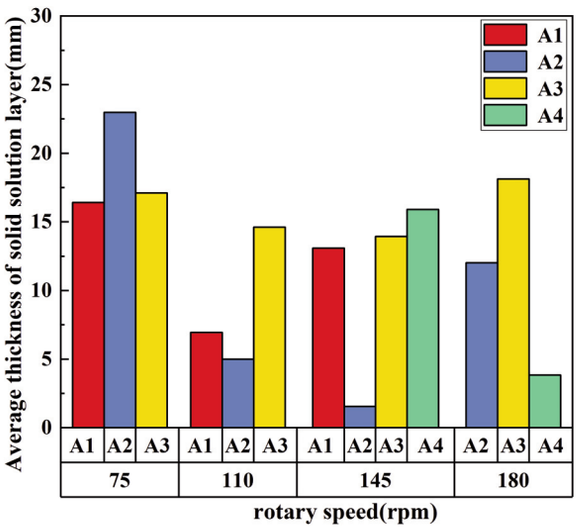

Figure 3. *The thickness change of solid solution layer at lime-slag dynamic reaction interface under different rotation rates*

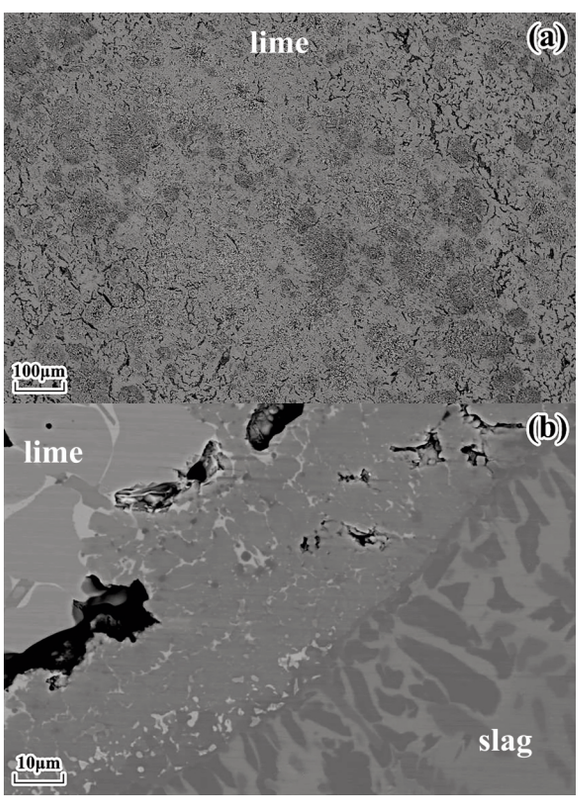

Figure 4. *(a) Microscopic morphology of lime at 75rpm in A4 slag; (b) Microscopic morphology of lime and slag reaction interface at 110rpm in A4 slag*

the reaction interface between slag A3 and lime at a rotation rate of 180 rpm. The average thickness of the (Ca, Mg, Fe) olivine layer initially increased and then decreased with the increase of the rotation rate when the rotation rate was 75-145 rpm. When the rotation rate was 110 rpm, the maximum thickness reached 98.13 μm, which was the thickest of all (Ca, Mg, Fe) olivine layers. In the slag A4, the (Ca, Mg, Fe) olivine layer was only present at 145 rpm and 180 rpm, which corresponded to the same mechanism, as the solid solution exists only at these two rotation rates. Their average thickness was 48.08 μm and 51.32 μm, respectively.

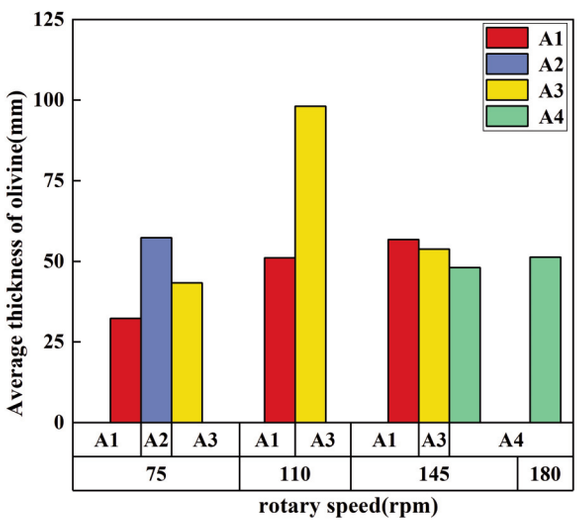

Figure 5. *Thickness change of (Ca, Mg, Fe) olivine layer at lime-slag interface under different rotation rates*

When lime and slag reacted at 1400°C at different rotation rates, the average thickness of the C_2S layer generated at the lime-slag interface changed with the rotation rate, as shown in Figure 6. In slag A2, the C_2S layer was formed at the lime-slag reaction interface at different rotation rates. The average thickness of the C_2S layer in slag A2 initially decreased and then increased with the increase of rotation rate. The maximum and minimum values were 24.17 μm and 2.32 μm, respectively, at the rotation rate of 75 rpm and 145 rpm. In slag A1, C_2S layer is not formed at the lime-slag reaction interface at 180 rpm. At 75 rpm to 145 rpm, the average thickness of the generated C_2S layer decreased with the increase of the rotation rate. In the slag A3, the C_2S layer was formed at 75 rpm and 110 rpm, and the average thickness of the produced C_2S was 8.92 μm and 25.08 μm, respectively. In slag A4, the C_2S layer was formed at 145 rpm and 180 rpm, and their average thickness was 26.83 μm and 8.81 μm, respectively.

When lime and slag reacted at 1400°C at different rotation rates, the average thickness of the C_3S layer generated at the lime-slag reaction interface changed with the rotation rate, as shown in Figure 7. When the rotation rate ranged from 75 rpm to 110 rpm, the

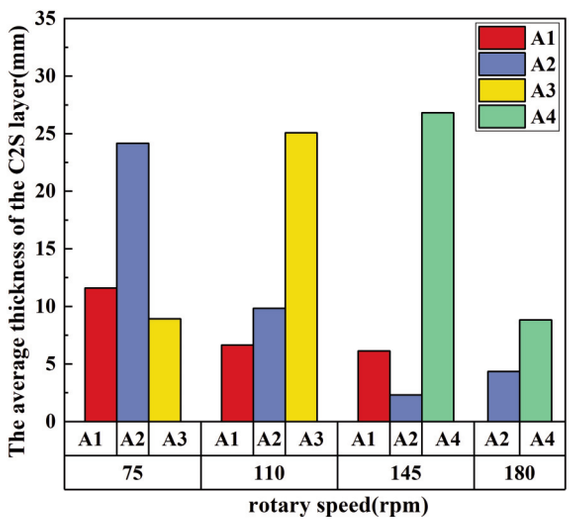

Figure 6. *The thickness change of C_2S layer at lime-slag interface under different rotation rates*

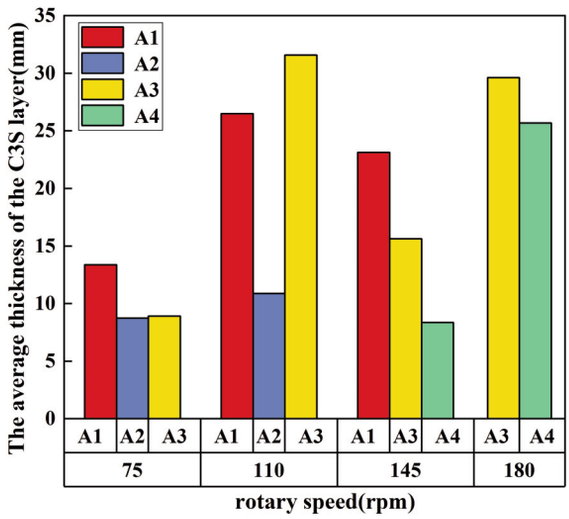

Figure 7. *The thickness change of C_3S layer at lime-slag interface under different rotation rates*

average thickness of the C_3S layer generated in the slag A1 to A3 showed a gradual increase with the increase of the rotation rate. At this point, there was no C_3S layer in A4, which was also due to the relatively slow mass transfer, which led to the overburning of lime. When the rotation rate was from 145 rpm to 180 rpm, the average thickness of the C_3S layer in slag A3 and slag A4 was similar and increased with the increase of rotation speed. However, no C_3S layer was formed in slag A2, and a thickness of 23.13 μm was formed in slag A1 at 145 rpm. Of all the slags, the average thickness of the C_3S formed by slag A3 at 110 rpm was the maximum, which was 31.58 μm.

The radius reduction of the lime particles after the static dissolution of lime in slags A1-A4 for 90 s is shown in Table 3. The volume *V* and the surface area *S* of the wall of the lime cylindrical particles used in this test can be expressed by the following equations (1) and (2) [9]:

$$V = \pi r^2 h \tag{1}$$

$$S = 2\pi r h \tag{2}$$

where *r* is the radius of lime particle, m; *h* is the height of lime particles, m.

The dissolution rate of active lime in slag *Vr* can be defined as the dissolution volume per unit area within a certain time [10-11], that is, formula (3) :

$$V_r = -\frac{1}{s}\frac{dV}{dt} = -\frac{dr}{dt} \tag{3}$$

where *Vr* is lime dissolution rate, m/s; *dr* is reduction value of lime radius, m; *dt* is lime dissolution time, s.

Substituting the data from Table 3 into Equation (3), the relationship diagram of the lime dissolution rate in slag A1 to A4 at different rotation rates can be obtained, as shown in Figure 8. When lime was dissolved in slag A1 to A4 for 90 s at different rotation rates, the dissolution rate increased linearly with the increase of rotation rate. Among them, the growth trend in slag A1 was particularly significant, while in slag A2, A3 and A4 the growth trend was slower. When the rotation rate was increased from 75 rpm to 180 rpm, the dissolution rate of lime in slag A1 continuously increased from 4.8×10^{-6} m/s to a maximum of 20.54×10^{-6} m/s. In slag A2, the dissolution rate of lime gradually increased from 2.52×10^{-6} m/s to 7.86×10^{-6} m/s. In slag A3, the dissolution rate of lime gradually increased from 4.51×10^{-6} m/s to 9.38×10^{-6} m/s. In slag A4, the dissolution rate of lime gradually increased from 3.06×10^{-6} m/s to 5.53×10^{-6} m/s. When the rotation rate was 75 rpm, the dissolution rate was A1 > A3 > A4 > A2, and the minimum and maximum values were 2.25×10^{-6} m/s and 4.8×10^{-6} m/s, respectively. When the rotation rate gradually increased from 110 rpm to 180 rpm, the dissolution rate was A1 > A3 > A2 > A4.

Table 3. *The radius reduction value ($r \times 10^4$ m) of lime dissolved in slag at different rotation rates for 90 s*

rate \ slag	A1	A2	A3	A4
75 rpm	4.28	2.27	4.06	2.76
110 rpm	9.33	4.75	5.80	3.89
145 rpm	14.41	6.45	6.93	3.90
180 rpm	18.49	7.08	8.45	4.98

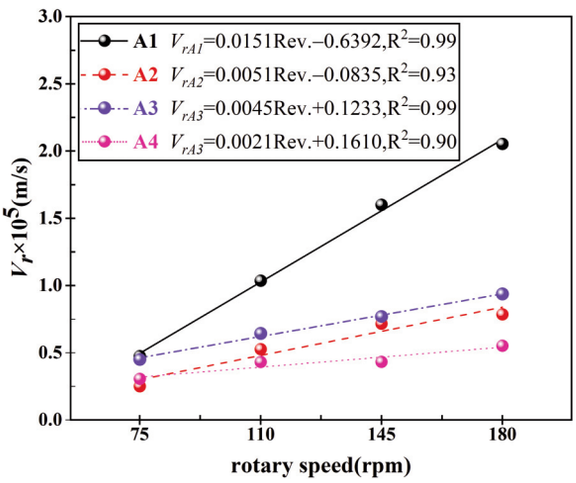

Figure 8. *Dissolution rate of lime in slag A1-A4 at 90 s under different rotation rates*

4. Discussion

The dissolution process of lime in the slag of CaO-Fe_tO-SiO_2-MgO based system conforms to the unreacted core model. The lime after rapid calcination is added to the slag, the lime is enveloped by liquid slag. The slag penetrates into the lime along the cracks and micropores formed during the calcination, so as to carry out the lime-slag interface reaction. Due to the fast diffusion rate of FeO in the slag, FeO will react with CaO first and form a CaO-FeO solid solution. When a continuous solid solution with a certain thickness is formed, SiO_2 with a slower diffusion rate is blocked outside the solid solution layer. In the solid solution layer, the CaO contained in the lime diffuses to the slag and reacts with MgO, FeO and SiO_2 in the slag to form (Ca, Mg, Fe) olivine and calcium-iron olivine. Since magnesium olivine and iron olivine can form infinite solid solutions, the chemical formula of olivine can be simply expressed as 3(Ca, Mg, Fe)O·SiO_2. As the lime-slag interface reaction continues, a concentration gradient is formed at the reaction interface. The FeO concentration first increases from the slag to (Ca, Mg, Fe) olivine phase to the CaO-FeO solid solution, then decreases and increases again, and finally accumulates in the CaO-FeO solid solution layer. The concentration difference is the driving force, and FeO diffuses from the slag and CaO-FeO solid solution layers into the (Ca, Mg, Fe) olivine phase and lime, respectively. The CaO concentration gradient formed by lime and slag promotes the diffusion of CaO from lime to slag, thus making the reaction proceed continuously. When the content of SiO_2 in the slag is high, the free SiO_2 in the slag cannot react completely with the CaO provided by the lime. At this point, the CaO reacts with the generated (Ca, Mg, Fe) olivine, resulting in the formation of low melting point calcium-magnesite facies containing MgO in the slag [12-14]. With the increase of the CaO content in the slag, the production of solid solutions also increases. Due to the slow diffusion rate of SiO_2, the amount of olivine (Ca, Mg, Fe) in the slag also gradually increases, resulting in a gradual thickening of the solid solution layer. Lime continuously dissolves in the slag, so that the content of CaO in the slag increases, and reacts with FeO to form a solid solution, resulting in the decrease of FeO content. It should be noted that CaO can not only react with SiO_2 to form a variety of silicates, but also continue to replace MgO in the calcium magnesium silicate ore phase when the FeO content is less than 20%, generating C_2S with a melting point of up to 2130°C and a dense structure [15]. The formation of C_2S requires the consumption of calcium-magnesite ore phase, so the thickness of CaO-FeO solid solution layer will be reduced. Finally, a dense layer of C_2S forms on the surface of the lime particles, which prevents the reaction from continuing and prevents dissolution. The content of undissolved lime particles in the slag will also continue to increase, resulting in the increase of the undissolved *f*-CaO content in the slag [16-19].

The dissolution rate is controlled by the mass transport of solutes in the slag layer around the lime. Forced convection dissolution of cylindrical lime in slag can be expressed as equation (4):

$$V_r = aU^b \tag{4}$$

where a and b are constants and *U* is the flow rate. In Figure 9, the relationship between *Vr* and *U* is

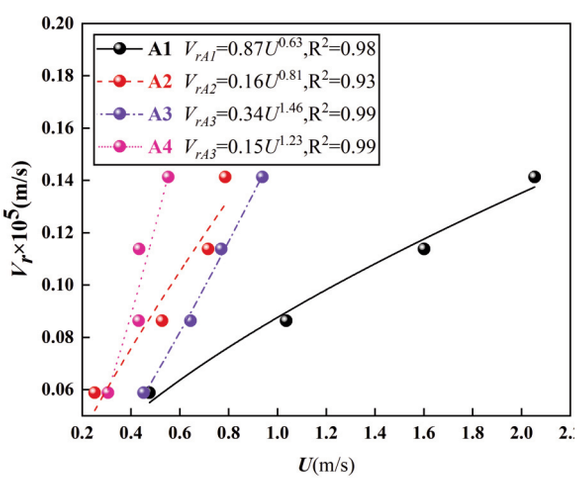

Figure 9. *The relationship between the dissolution rate of lime and the flow rate at different rotation rates when the lime is dissolved in the slag A1-A4 for 90 s*

drawn. The values of b in four kinds of slag were calculated as 1.82, 2.17, 1.61 and 2.30 respectively. According to the results, it is concluded that under the present experimental conditions, the rate control step of dissolution is the diffusion of solute in the boundary layer of slag.

When mass transport in the liquid boundary layer is the rate control step, the mass flux J can be expressed by the following equation (5):

$$J = k(n_s - n_b) \tag{5}$$

where k is the mass transfer coefficient, n is the mass density of the solute in the liquid slag, and the subscript s and b represent the amount at the liquid interface and volume, respectively. In addition, the relationship between J and the dissolution rate Vr of the solid lime cylinder can be derived from the mass balance of CaO at the reaction interface, as shown in equation (6):

$$\rho_{CaO} A V_r = AJ \tag{6}$$

where ρ_{CaO} is the apparent mass density of lime, and A is the interface area. The mass transfer coefficient k in the liquid phase can be obtained by equation (7), namely:

$$k = (100\rho_{CaO} V_r) / [\rho_{slag} \Delta(mol\%CaO)] \tag{7}$$

According to equation (7), the mass transfer coefficient of the dynamic dissolution of lime in slag A1-A4 for 90 s at different rotation rates can be obtained, as shown in Table 4:

Table 4. *Mass transfer coefficient of lime dissolution in slag A1 to A4 for 90 s at different rotation rates ($k \times 10^5$ m/s)*

slag / rate	A1	A2	A3	A4
75 rpm	1.70	1.08	2.80	4.15
110 rpm	3.70	2.26	4.00	5.86
145 rpm	5.72	3.08	4.78	5.88
180 rpm	7.33	3.38	5.83	7.50

According to the data in Table 4, the mass transfer coefficient changes during the dynamic dissolution of lime in the slag from A1 to A4 for 90 s at 1400°C at different rotation rates can be obtained, as shown in Figure 10. The mass transfer coefficient k of lime in different slag at different rotation rates shows a general trend of increasing with the increase of rotation rate when the slag changes from A1 to A4. The mass transfer coefficients reached the maximum when the rotation rate was 180 rpm, which were 7.33×10^5 m/s, 3.38×10^5 m/s, 5.83×10^5 m/s and 7.50×10^5 /s, respectively. The mass transfer coefficient is generally A4 > A1 > A3 > A2.

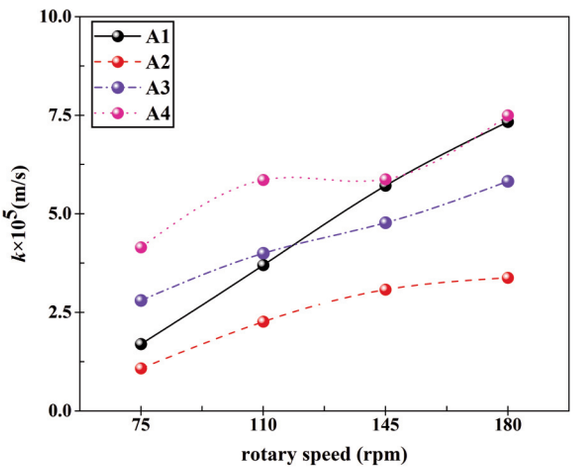

Figure 10. *The average mass transfer coefficient of lime dynamically dissolved in slag A1 to A4 at different rotation rates for 90 s*

On the other hand, the influence of flow conditions on mass transfer rate is evaluated quantitatively by using dimensionless correlation, as shown in equation (8):

$$J_D = StSc^a = C\,\mathrm{Re}^b \tag{8}$$

where J_D is the dimensionless number, St is the Stanton number, Sc is the Schmidt number, and Re is the Reynolds number, where a is usually 2/3 and b is a constant. The relationship between Re and J_D can be obtained as shown in Figure 11.

When a rotating cylinder is used at a shallower immersion depth, the Levich-Cochran equation is best

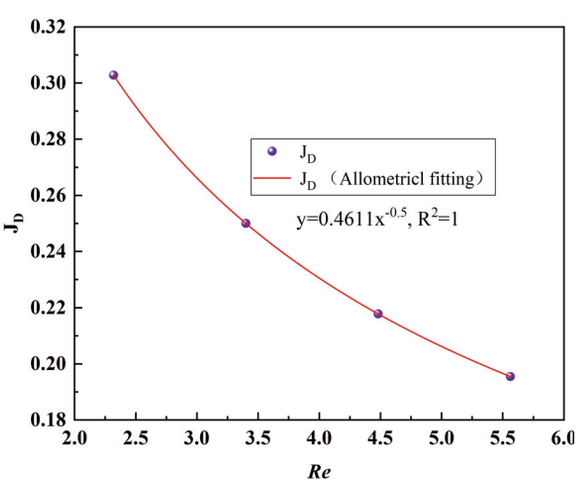

Figure 11. *The relationship between J_D and Re*

used to describe the mass transfer of a rotating disk:

$$\delta = 1.61(\frac{D}{\nu})^{1/3}(\frac{\nu}{\omega})^{1/2} \quad (9)$$

The formula is applicable to $v/D >> 1$ and $10 < r^2\omega/v < 10^4$, where δ is the thickness of the concentration boundary layer, v is the kinematic viscosity of the solvent, $v=\eta/\rho_{CaO}$. η is the slag viscosity, and the calculated results according to FactSage 8.1 are shown in Table 5. ω is the angular velocity of the rotating disk, and $\omega=2n\pi$ is the rotational speed. D is the diffusion coefficient of the dissolved substance, $D=\delta k$.

Table 5. *Experimental calculation results*

slag	U/mm·s^{-1}	η/Pa·s^{-1}	D/×102mm^2·s^{-1}	δ/×10mm
A1	58.88	0.15	1.12	6.59
	86.35	0.15	2.70	7.30
	113.83	0.15	4.22	7.38
	141.3	0.15	5.21	7.11
A2	58.88	0.23	0.63	5.86
	86.35	0.23	1.44	6.36
	113.83	0.23	1.86	6.03
	141.3	0.23	1.81	5.37
A3	58.88	0.15	2.37	8.47
	86.35	0.15	3.04	7.60
	113.83	0.15	3.22	6.75
	141.3	0.15	3.69	6.33
A4	58.88	0.20	4.61	11.09
	86.35	0.20	5.79	9.89
	113.83	0.20	4.73	8.05
	141.3	0.20	5.79	7.73

The CaO diffusion coefficient in this paper is estimated by equation (10) by combining equation (7) with Levich-Cochran equation:

$$D^{2/3} = \frac{161\rho_{slag}V_r\nu^{1/6}}{\omega^{1/2}\rho_{CaO}\Delta(mol\%CaO)} \quad (10)$$

The equation for δ can be derived from equation (6):

$$\delta = \frac{1}{C}\cdot \mathrm{d}\cdot \mathrm{Re}^{-(1+b)}\cdot Sc^{(a-1)} \quad (11)$$

Substitute equation (10) into equation (7) to get:

$$\mathrm{k} = C\cdot U^{b+1}\cdot \mathrm{d}^{\mathrm{b}}\cdot \eta^{-(a+b)}\cdot \rho_{CaO}{}^{(a+b)}\cdot D^{\mathrm{a}} \quad (12)$$

Regression analysis in Figure 11 shows that:

$$J_D = 0.4611\mathrm{Re}^{-0.5} \quad (13)$$

$$\delta = 32.53\mathrm{Re}^{-0.5}\cdot Sc^{-1/3} \quad (14)$$

$$\mathrm{k} = 0.4611U^{0.5}\cdot \mathrm{d}^{-0.5}\cdot \eta^{-1/6}\cdot \rho_{CaO}{}^{1/6}\cdot D^{2/3} \quad (15)$$

5. Conclusion

(1) In the early and middle stages of the CaO-Fe_tO-SiO_2-MgO system, when the lime reacts with the slag dynamically and the rotation rate changes, in addition to CaO-FeO solid solution, (Ca, Mg, Fe) olivine and C_2S, C_3S is also generated. C_3S is formed by the reaction of C_2S and CaO dissolved in high temperature liquid phase. At the same time, C_3S can also be formed by the direct reaction of SiO_2 and CaO.

(2) When lime is dissolved in slag A1 to A4 with different composition for 90 s under different rotation rates at 1400°C, the dissolution rate increases linearly with the increase of rotation rate. Among them, the growth trend in slag A1 is particularly significant, while the growth trend in slag A2, A3 and A4 is slower.

(3) The average mass transfer coefficient k of dynamic dissolution of lime in slag at 1400°C increases with the increase of rotation rate when the slag changes from A1 to A4. The mass transfer coefficient reached its maximum at a rotation rate of 180 rpm, which were 7.33×10^5 m/s, 3.38×10^5 m/s, 5.83×10^5 m/s and 7.50×10^5 m/s, respectively. The overall mass transfer coefficient is A4 > A1 > A3 > A2.

(4) Based on the dissolution of lime in different components of the slag in CaO-Fe_tO-SiO_2-MgO system at 1400°C, the calculation formulas for lime k and δ are derived based on this experiment:

$$\delta = 32.53\mathrm{Re}^{-0.5}\cdot Sc^{-1/3} \quad (16)$$

$$\mathrm{k} = 0.4611U^{0.5}\cdot \mathrm{d}^{-0.5}\cdot \eta^{-1/6}\cdot \rho_{CaO}{}^{1/6}\cdot D^{2/3} \quad (17)$$

Acknowledgments

This work was financially supported by the National Natural Science Foundation of China (52074199), and Hubei Central Guide Local Science and Technology Development Project (2023EGA040).

Author Contributions

J.-L. Li: Conceptualization, Funding acquisition, Investigation, Methodology, Validation, Visualization, Writing - original draft. C. Jia: Methodology, Software, Writing - original draft, Validation. Q.-Q. Mou: Validation, Writing - original draft. M.-X.

Zhang: Validation, Writing - original draft. R. A. Muvunyi: Validation. Y. Yu: Validation.

Data availability Statement

The data cannot be made publicly available upon publication because they are not available in a format that is sufficiently accessible or reusable by other researchers. The data that support the findings of this study are available upon reasonable request from the authors.

Conflict of Interest

The authors declare that they have no conflict of interest.

References

[1] H. Matsuura, X. Yang, G.Q. Li, Z.F. Yuan, F, Tsukihashi, Recycling of ironmaking and steelmaking slags in Japan and China, International Journal of Minerals, Metallurgy and Materials, 29(4) (2022) 739-749. https://doi.org/DOI: 10.1007/s12613-021-2400-5

[2] Y.Z. Li, X.H. Li, Y.Q. Sun, X.M. Shen, P. Fan, W.H. Cheng, Experimental study on dissolution rate of CaO into liquid slag of Cao-MgO-FetO-SiO_2, Ironmaking and Steelmaking, 28(10) (1993) 18-23. https://doi.org/DOI:10.13228/j.boyuan.issn0449-749x.1993.10.005

[3] M.X. Zhang, J.L. Li, C. Jia, Y, Yu, X, Xie, Evolution of interface characteristic between quicklime and CaO-SiO_2-FetO-MgO melt during slag-forming procedure in converter under different times, Steel Research International, 94(12) (2023). https://doi.org/DOI: 10.1002/SRIN.202370125

[4] Y.J. Xia, X.P. Li, J. Li, D.D. Fan, Dissolution behavior of lime particles in CaO-FeO-SiO_2-P_2O_5 Slag, The Chinese Journal of Process Engineering, 17(05) (2017) 1041-1046. https://doi.org/DOI: 10.12034/j.issn.1009-606X.217121

[5] N. Maruoka, A. Ishikawa, H. Shibata, S. Kitamura, Dissolution rate of various limes into steelmaking slag, High Temperature Materials and Processes, 32(1) (2013) 15-24. https://doi.org/DOI:10.1515/htmp-2012-0049

[6] T. Deng, J. Gran, S.C. Du, Dissolution of lime in synthetic 'FeO'-SiO_2 and CaO-'FeO'-SiO_2 slags, Steel Research International, 81(5) (2010) 347-355. https://doi.org/DOI:10.1002/srin.201000017

[7] N. K. Arakere, Gigacycle rolling contact fatigue of bearing steels: A review, International Journal of Fatigue, 93 (2016) 23. https://doi.org/10.1016/j.ijfatigue.2016.06.034.

[8] M. Matsushima, S. Yadoomaru, K. Mori, Y. Kawai, A Fundamental study on the dissolution rate of solid lime into liquid slag, Transactions of the Iron and Steel Institute of Japan, 17(8) (1977) 442-449. https://doi.org/DOI:10.2355/isijinternational1966.17.442

[9] N. Maruoka, A. Ito, M. Hayasaka, S. Kitamura, H. Nogami,Enhancement of quicklime dissolution in steelmaking slags by utilizing residual CO_2 from quicklime, ISIJ International, 57(10) (2017) 1677-1683. https://doi.org/DOI:10.2355/isijinternational.ISIJINT-2017-103

[10] I.Z. Yildirim, M. Prezzi, Chemical, mineralogical, and morphological properties of steel slag, Advances in Civil Engineering, 1(2011) 1-13. https://doi.org/DOI: 10.1155/2011/463638

[11] W.Y. Yang, C.J. Zheng, K. Du, H. Chen, J. Cui, C.L. Xu, X.F. Jiang, metallurgical reactions in steelmaking process for 300 t BOF, Journal of Iron and Steel Research, 12(S1) (2000) 22-26. https://doi.org/DOI:10.13228/j.boyuan.issn1001-0963.2000.s1.005

[12] J. Martinsson, B. Glaser, S.C. Du, Lime dissolution in foaming BOF slag, Metallurgical and Materials Transactions B, 49(6) (2018) 3164-3170. https://doi.org/DOI: 10.1007/S11663-018-1421-6

[13] R.O. Russell, Lime reactivity and solution rates, JOM, 19(8) (1967) 104-106. https://doi.org/DOI: 10.1007/bf03378628

[14] W.W. Mao, C.X. Li, H. Lu, H. Li, W. Xie, Limestone dissolution and decomposition in steelmaking slag, Ironmaking and Steelmaking, 45(8) (2018) 720-726. https://doi.org/DOI: 10.1080/03019233.2017.1326549

[15] H.D. Meng, L. Liu, Petrographical study on slag formation in the process of converter steelmaking, Ironmaking and Steelmaking, 45(06) (2010) 26-30. https://doi.org/DOI:10.13228/j.boyuan.issn0449-749x.2010.06.009

[16] S. Amini, M. Brungs, O. Ostrovski, Dissolution of dense lime in molten slags under static conditions, ISIJ International, 47(1) (2007) 32-37. https://doi.org/DOI: 10.2355/isijinternational.47.32

[17] D. Senk, H.W. Gudenau, S. Geimer, E. Gorbunova, Dust injection in iron and steel metallurgy, ISIJ International, 46(12) (2006) 1745-1751. https://doi.org/DOI: 10.2355/isijinternational.46.1745

[18] J. Yang, M. Kuwabara, T. Asano, A. Chuma, J. Du, Effect of lime particle size on melting behavior of lime-containing flux, ISIJ International, 47(10) (2007) 1401-1408. https://doi.org/DOI: 10.2355/isijinternational.47.1401

[19] M.X. Zhang, J.L. Li, S.N. Li, H.Y. Zhu, Evolution behaviour of interfacial structure between quicklime and converter slag: slag-forming route based on FetO component, Ironmaking and Steelmaking, 50(1) (2023) 101-108. https://doi.org/DOI: 10.1080/03019233.2022.2088158

EFEKAT BRZINE ROTACIJE NA RASTVARANJE KREČA U SISTEMU CaO-Fe_tO-SiO_2-MgO

C. Jia [a], Q.-Q. Mou [b], Y. Yu [c], R. A. Muvunyi [a], M.-X. Zhang [a], J.-L. Li [a, c, *]

[a] Provincijska ključna laboratorija za nove procese proizvodnje gvožđa i čelika, Univerzitet nauke i tehnologije u Vuhanu, Vuhan, provincija Hubej, Kina
[b] CNCEC-EEC Dajiang Tehnologija za zaštitu životne sredine Co., LTD., Huangši, provincija Hubej, Kina
[c] Ključna laboratorija za metalurgiju gvožđa i iskorišćenje resursa Ministarstva obrazovanja, Univerzitet nauke i tehnologije u Vuhanu, Vuhan, provincija Hubej, Kina

Apstrakt

Za proces konvertorske proizvodnje čelika, nepotpuno rastvoreni kreč prisutan je u čeličnoj šljaci u obliku f-CaO, što smanjuje stepen iskorišćenja metalurške šljake i dovodi do rasipanja resursa. Izuzetno je važno smanjiti proizvodnju f-CaO u šljaci i podstaći brzo i potpuno rastvaranje kreča. Ovaj rad se bazira na ranim i srednjim fazama formiranja šljake u konvertoru, uzimajući u obzir CaO komponentu. Brzina rastvaranja kreča u četiri različite šljake ispitana je metodom rotirajuće šipke. Ponašanje na granici kreč-šljaka i promene u brzini rastvaranja kreča proučavani su pomoću rendgenske difrakcije i elektronske sonde mikroanalizatora. Eksperimentalni rezultati pokazuju da se CaO-FeO čvrsta rastvorna faza i (Ca, Mg, Fe) olivin formiraju kada kreč reaguje s tečnom šljakom na 1400°C. Kada se sadržaj FeO smanji, CaO reaguje sa kalcijum-magnezijum-silikatom i formira sloj $2CaO{\cdot}SiO_2$ visoke tačke topljenja i velike gustine. Pored toga, pri različitim brzinama rotacije, formira se sloj $3CaO{\cdot}SiO_2$ između sloja CaO-FeO čvrste rastvorne faze i sloja C_2S. Kako se brzina rotacije povećava, brzina rastvaranja kreča takođe raste, a koeficijent prenosa mase dostiže maksimum pri brzini rotacije od 180 obrtaja u minuti. Maksimalne vrednosti iznose $20{,}54\times10^{-6}$ m/s, $7{,}86\times10^{-6}$ m/s, $9{,}38\times10^{-6}$ m/s i $5{,}53\times10^{-6}$ m/s.

Ključne reči: *Kreč; Reakcioni interfejs; $2CaO{\cdot}SiO_2$; Brzina rastvaranja; Prenos mase*